

Compatibility Analysis of Piezoelectric Actuators in Supercritical Carbon Dioxide

Chunmeng Xu

*School of Electrical and Computer Engineering
Georgia Institute of Technology
Atlanta, Georgia, USA
chunmengxu@gatech.edu*

Jia Wei

*School of Electrical and Computer Engineering
Georgia Institute of Technology
Atlanta, Georgia, USA
jia.wei@gatech.edu*

Lukas Gruber

*School of Electrical and Computer Engineering
Georgia Institute of Technology
Atlanta, Georgia, USA
lukas.gruber@ece.gatech.edu*

Abstract— The compatibility of a multilayer piezoelectric actuator operating in supercritical carbon dioxide was tested using a voltage-based self-sensing technique. The phase transitions of carbon dioxide to supercritical state were recorded visually. No degradation was observed in leakage current of the piezoelectric actuator after being immersed in supercritical carbon dioxide for hours. This confirmed compatibility allows further applications of supercritical carbon dioxide as the insulating medium in power equipment, like a fast mechanical switch for hybrid direct current circuit breakers in medium voltage direct current power systems.

Keywords—*fast mechanical switch; hybrid circuit breaker; medium voltage direct current; piezoelectric actuator; supercritical fluids; ultrafast disconnect switch;*

I. INTRODUCTION

A. Background

Supercritical fluids have been proposed as a potential replacement of SF₆ gas in electrical equipment [1, 2]. Their potential as a novel insulation medium is currently being explored [3]. Supercritical carbon dioxide (scCO₂, Fig. 1(a)), as the most widely studied type of supercritical fluid so far, is believed to combine the advantages of both gas dielectrics and liquid dielectrics and becomes an insulating medium with low viscosity, high dielectric strength, and high thermal conductivity [4]. Therefore, the scCO₂ is especially suitable for the insulation among small gaps. For example, a 0.1 mm gap with scCO₂ (8 MPa, 310 K) could withstand 18 kV direct current (DC) voltage [5], which is already the voltage level of a typical medium-voltage DC power system. In our application, the scCO₂ is chosen as the insulating medium of a 12 kV-rated disconnect switch actuated by a piezoelectric actuator with 0.1 mm maximum travel curve (Fig. 1(b)).

Piezoelectric actuators utilize the deformations of piezoelectric ceramic under electric fields to actuate. These solid deformations are performed in a very swift and precise manner; a piezoelectric actuator typically has microsecond-level response speed with nanometer-level displacement resolution. Whereas, the displacement ranges of piezoelectric actuators are very limited, as most commercially available actuators' displacement ranges fall below 2 mm [6]. The piezoelectric actuator (Fig. 1(b)) chosen for our DC disconnect switch has 80 μ s of response time and 1.3 nm of resolution to achieve

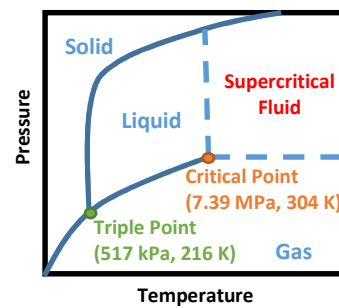
ultrafast switching, but the maximum no-load displacement is only 130 μ m. The high electric field at such a small spacing requires a powerful dielectric medium like scCO₂.

B. Literature Review

The combination of scCO₂ and piezoelectric actuators is quite an original approach and their mutual compatibility has not been reported in literature. The reliability analyses of piezoelectric actuator traditionally focus on the compatibility with water, as the moisture penetration is a major degradation mechanism for multilayer stack piezoelectric actuator [7-9]. The degradations of piezoelectric actuators in a high-humidity environment are mainly in the forms of reduced strain and increased leakage current [8]. Thus, these two parameters will also be monitored in this compatibility analysis.

C. Problem Statement

In this study, a multilayer stack piezoelectric actuator will be immersed inside CO₂ in both supercritical state and liquid state to test its compatibility. The online monitoring of actuator's operations under immersions will be achieved with voltage-based self-sensing technique, and this technique will be first calibrated with offline displacement measurements from high-precision displacement sensor. The transitions of CO₂ from liquid state to supercritical state will also be recorded visually.

(a) Simplified phase diagram of CO₂

(b) Piezoelectric actuator

Fig.1 Objects of research: (a) a simplified phase diagram of CO₂ that defines supercritical state; (b) photo of a multilayer piezoelectric actuator (Cedrat[®] PPA120XL)

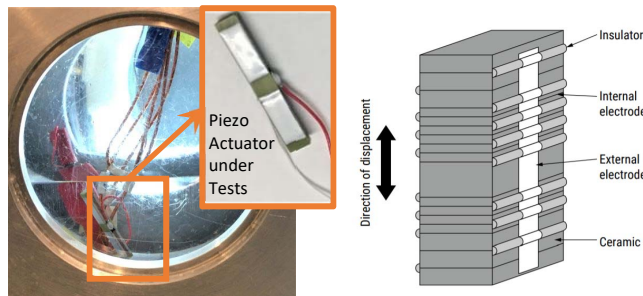
II. EXPERIMENTAL SETUP

There were two experimental setups in which the compatibility tests of the piezoelectric actuator were performed: one for calibrating the voltage-based self-sensing technique, the other for compatibility test with CO_2 immersion. Both setups used the same piezoelectric actuator and electric circuits for online monitoring.

A. Piezoelectric Actuator Under Tests

The piezoelectric actuator chosen for the 12 kV-rated fast mechanical switch is Cedrat® PPA120XL model (Fig. 1(b)), which has 130 μm maximum displacement. However, due to the availability, cost and size issues, a mini-size actuator of KEMET® AE0203D16DF model was used in immersion tests. Both models' piezoelectric ceramic stacks come from the same manufacturer so they are assumed to share similar compatibility with scCO_2 .

The KEMET® AE0203D16DF actuator has its physical structure as illustrated in Fig. 2 [10]. The ratings of this actuator are shown in Table I. The actuator is coated with resin as a standard industrial approach, whereas resin or polymer coating was found less effective in stopping moisture penetration that leads to performance degradation in the actuator. More effective protections are ceramic coating or metal-case encapsulation of the actuator [11].



(a) Piezo actuator in liquid CO_2 (b) Piezo actuator structure

Fig.2 Piezoelectric actuator (KEMET® AE0203D16DF) chosen for compatibility tests; (a) photo of actuator immersed inside liquid CO_2 ; (b) illustration of actuator's structure from product catalog [10]

TABLE I. RATINGS OF PIEZOELECTRIC ACTUATOR UNDER TEST

Part Number	AE0203D16DF	Dimensions	100 \times 20 \times 3 mm^3
Displacement	17.4 μm	Driving Voltage	0 – 150 V _{DC}
Capacitance	0.35 μF	Force Output	200 N
Insulation Resistance	50 M Ω	Resonant Frequency	69 kHz
Protection Measure	Resin coated	Temperature Range	-25 – 85 °C

B. Self-sensing Technique Calibration Setup

Voltage-based self-sensing technique has been chosen in this study to online monitor the displacement outputs of piezoelectric actuator while it is immersed inside scCO_2 . As indicated in Fig. 2(a), the size of high-pressure chamber containing scCO_2 is very limited, so a displacement sensor could

not fit into the chamber. If using a film-type strain gauge that attaches onto the surface of the piezoelectric actuator, the reliability of the strain gauge itself is not guaranteed in this high-pressure environment of scCO_2 . Therefore, a sensorless approach, also known as self-sensing approach, became more suitable in this study.

Voltage-based self-sensing means using driving voltage readings as the indicator of actuator's displacement value. So in the calibration stage, a relationship between actuator's driving voltages and externally-measured actuator's displacements was determined. The experimental setup to calibrate this voltage-displacement (V - d) relationship is shown in Fig. 3.

The calibration setup consists of eight components to perform three tasks: powering up the actuator with driving voltage and current monitoring (G, H, F, and D), sensing actuator's displacement (A, B, C, and D), and monitoring actuator's real-time capacitance values (E, G, and F). The voltage readings from (H) piezo driver and displacement readings from (B) eddy-current displacement sensor (Lion Precision® ECL101 amplifier with U5 probe, 10 kHz bandwidth, 9.6 nm resolution) were collected in real-time to the laptop through Labview® program. So the V - d relationship could be linearly fitted based on the collected data and it will be shown in Fig. 5.

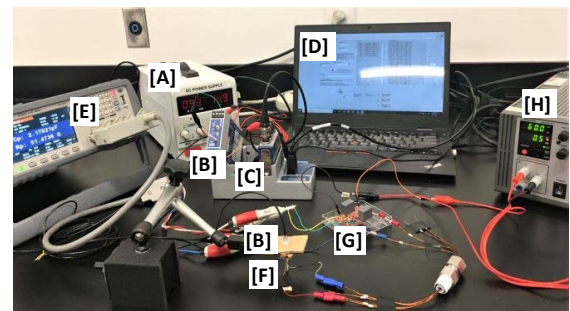


Fig.3 Calibration test setup to obtain voltage-displacement relationships for constructing voltage-based self-sensing technique

C. CO_2 Immersion Test Setup

The compatibility tests were performed in the CO_2 immersion test setup. The scCO_2 existed inside a self-designed (L) optical chamber with two-layer transparent windows (inner layer is chemically strengthened alkali-aluminosilicate glass, outer layer is polycarbonate), so the transitions between two-phase gas-liquid state and single-phase supercritical state could be clearly viewed through the window (as shown in Fig. 6).

There were phase transitions that happened in an isochoric manner during CO_2 immersion tests, that is, the total volume of

CO_2 is constant after the initial filling of CO_2 from (J) storage cylinder and the (N) valve was kept closed during tests. The temperature of optical chamber was controlled by (M) thermometer and heating tapes and it was set to 35.2°C . The CO_2 pressure was changed accordingly with CO_2 temperature, and the calculated pressure of sc CO_2 at 35.2°C was around 8 MPa with a density of about 500 kg/m^3 . The CO_2 used for tests was pure clean grade with 99.995% purity.

The piezoelectric actuator was fully immersed inside liquid-state CO_2 (LCO_2) and sc CO_2 during the tests. Both driving voltage and leakage current readings of actuator were recorded during voltage-controlled charging processes (0 V to 120 V), constant voltage processes (120 V) and uncontrolled discharging processes (120 V to 0 V) in air, LCO_2 and sc CO_2 states. The peripheral electrical connections during CO_2 immersion tests were kept the same as in the calibration setup.

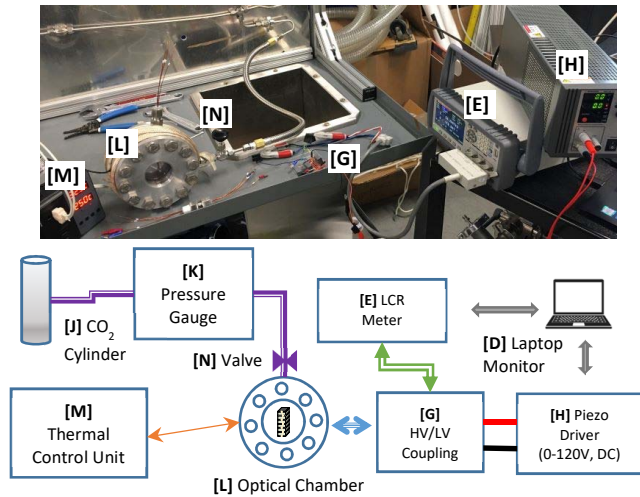


Fig.4 CO_2 immersion setup for compatibility tests

III. RESULTS AND DISCUSSIONS

A. Calibration of Voltage-based Self-sensing Technique

The piezoelectric actuator to be tested in CO_2 immersion test was first calibrated to find its V - d relationship. This linearized relationship was later used to calculate the real-time displacements of immersed actuator based on voltage readings.

As shown in Fig. 5(a), the actuator performed a complete expand/charge – stay – retract/discharge cycle under driving voltage of 0 V – 110 V – 0 V. As the displacement waveform synchronized with driving voltage waveform, they formed an XY plot as shown in Fig. 5(b). The color gradient in Fig. 5(b) shows the elapse of time, so the lower side of hysteresis corresponds to the expanding process and the upper side corresponds to the retracting process of actuator. There existed a hysteresis loop in the V - d curve which was caused by the energy storage nature of piezoelectric materials. A linearized V - d equation was fitted out of calibration readings as shown below:

$$d_{\text{actuator}}[\mu\text{m}] = 0.131 * V_{\text{actuator}}[\text{V}] - 0.00808 \quad (1)$$

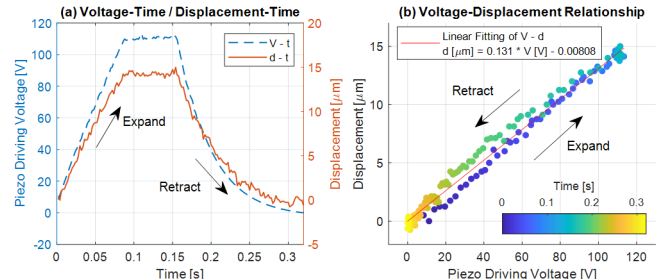


Fig.5 The time-domain displacements of actuator under corresponding driving voltages (left), then the V - d relationship was linearly fitted (right)

B. Transitions into Supercritical State

The major advantage of using the self-designed optical chamber is that the phase transitions of CO_2 can be monitored visually. A set of photos about CO_2 in different states during the CO_2 immersion test is shown in Fig. 6.

Depending on the chamber temperature, the CO_2 displayed different visual conditions. The liquid-state CO_2 filled into the optical chamber at 11°C and 4.6 MPa, there was a clear gas/liquid interface as shown in Fig. 6(a), and the operations of piezoelectric actuator in LCO_2 immersion were performed in this condition. Then, when the chamber temperature arose to 28°C , the liquid part of CO_2 calmly turned into opaque without vigorous bubble forming like evaporation (Fig. 6(b)), this was the transitional period to supercritical state. Once the chamber temperature approaches critical temperature of 31°C , the gas/liquid interface blurred and dropped, and a hint of smoke-like fog slowly spread into the gas state (Fig. 6(c)). This fog was possibly made of molecule clusters – a unique gathering of molecules existed in the supercritical state. Finally, the inner chamber space was fully occupied by sc CO_2 as the gas/liquid interface disappeared in Fig. 6(d), and a critical opalescence was reached as it was clouded inside the chamber.

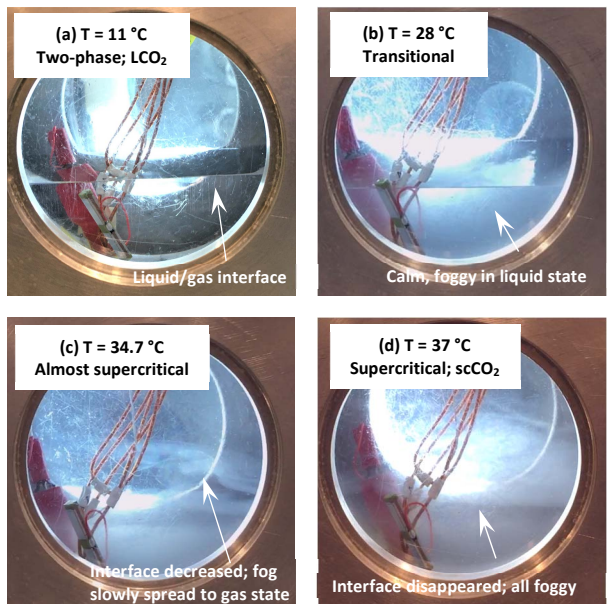


Fig.6 Visual records of phase transitions of CO_2 during CO_2 immersion test in the optical chamber

C. Operations of Piezoelectric Actuator in $scCO_2$ and LCO_2

The piezoelectric actuator was operated under similar driving voltages shown in Fig. 5(a). The $scCO_2$ readings were collected after one hour of $scCO_2$ immersion, and the LCO_2 readings were collected with liquid-state CO_2 immersion. The displacement values shown in Fig. 8 were calculated with Eq.(1), which was the derived relationship from the voltage-based self-sensing technique.

As indicated in Fig. 7 and 8, the voltage, current and displacement readings of piezoelectric actuator during voltage ramping up or down processes did not have noticeable differences among air, $scCO_2$ or LCO_2 immersion. The variances in leakage current readings under constant 120 V excitation were within standard deviation ranges. Therefore, it was experimentally determined that the short-time influence of $scCO_2$ immersion or LCO_2 immersion for the piezoelectric actuator under test was negligible.

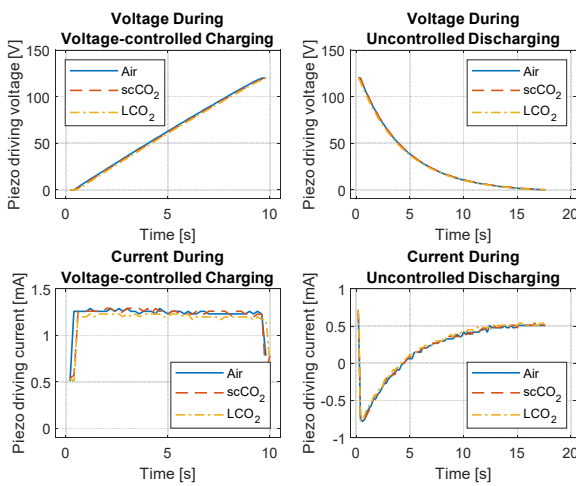


Fig.7 Online-monitored driving voltage and current readings of piezoelectric actuator in air, $scCO_2$ and LCO_2 states

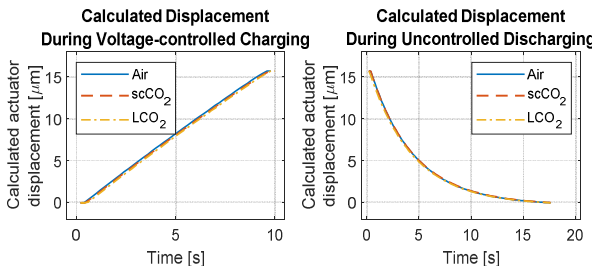


Fig.8 Calculated displacements of piezoelectric actuator in air, $scCO_2$ and LCO_2 states according to Eq.(1)

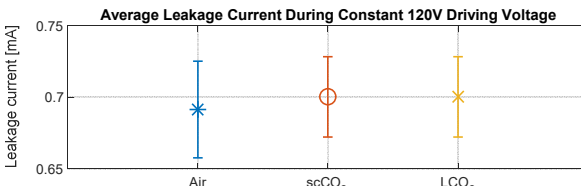


Fig.9 Online measured leakage current of piezoelectric actuator during constant 120 V voltage excitation in air, $scCO_2$ and LCO_2 immersions

IV. CONCLUSION AND FUTURE WORK

Reliable operations of a multilayer piezoelectric actuator have been performed in both supercritical and liquid carbon dioxide environment after short-time immersion. Driving voltage and leakage current values obtained through online monitoring during carbon dioxide immersion have been compared to assess the short-time compatibility. The piezoelectric actuator's real-time displacement values during immersion were also calculated with calibrated voltage-based self-sensing technique.

There are several directions of future work planned. As this study confirmed the short-time compatibility, long-time reliability needs to be checked before constructing a disconnect switch whose expected lifetime goes beyond several years. Moreover, the resolution and accuracy of voltage-based self-sensing technique are quite limited, the capacitance-based self-sensing technique will be considered based on the data obtained from the LCR meter in both setups.

ACKNOWLEDGMENT

This work has been funded in part by ARPA-E grant DE-AR0001113. Authors would like to especially thank Dr. Alfredo Vazquez Carazo from Micromechatronics Inc. for his expertise on piezoelectric actuator selections and operations.

REFERENCES

- [1] Y. Tian, J. Wei, C. Park, Z. Wang, and L. Gruber, "Modelling of electrical breakdown in supercritical CO_2 with molecular clusters formation," in *International Conference on the Properties and Applications of Dielectric Materials*, 2018, pp. 992-995.
- [2] E. J. M. v. Heesch *et al.*, "Proposing supercritical fluids as a replacement for SF₆ in high-voltage power switches: Gas discharges in supercritical fluids for make and break operation," in *IEEE International Power Modulator and High Voltage Conference 2016*, pp. 312-314.
- [3] E. J. M. v. Heesch *et al.*, "Supercritical fluids for high-power switching," in *IEEE International Power Modulator and High Voltage Conference*, 2014, pp. 126-129.
- [4] J. Zhang *et al.*, "Breakdown strength and dielectric recovery in a high pressure supercritical nitrogen switch," *IEEE Transactions on Dielectrics and Electrical Insulation*, vol. 22, no. 4, pp. 1823-1832, 2015.
- [5] J. Wei, A. Cruz, C. Xu, F. Haque, C. Park, and L. Gruber, "A Review on Dielectric Properties of Supercritical Fluids," in *IEEE Electrical Insulation Conference*, 2020.
- [6] C. Xu, T. Damle, and L. Gruber, "A Survey on Mechanical Switches for Hybrid Circuit Breakers," in *IEEE Power & Energy Society General Meeting*, 2019, pp. 1-5.
- [7] S. Yoshikawa and M. Farrell, "Actuator environmental stability," in *Smart Structures and Materials 2000: Smart Structures and Integrated Systems*, 2000, vol. 3985, pp. 652-659: International Society for Optics and Photonics.
- [8] M. Kuna, "Fracture mechanics of piezoelectric materials – Where are we right now?," *Engineering Fracture Mechanics*, vol. 77, no. 2, pp. 309-326, 2010.
- [9] J. Thongrueng, T. Tsuchiya, and K. Nagata, "Lifetime and Degradation Mechanism of Multilayer Ceramic Actuator," *Japanese Journal of Applied Physics*, vol. 37, no. Part 1, No. 9B, pp. 5306-5310, 1998.
- [10] KEMET, "Multilayer Piezoelectric Actuators - AE Series Resin Coated," KEMET, Ed., ed, 2018.
- [11] P. Pertsch, B. Broich, R. Block, S. Richter, and E. Hennig, "Development of Highly Reliable Piezo Multilayer Actuators and Lifetime Tests under DC and AC Operating Conditions," ed: PI Ceramic GmbH, 2010.